Cell Reports, Volume *34*

Supplemental information

Transcriptional programming drives Ibrutinib-resistance evolution in mantle cell lymphoma

Xiaohong Zhao, Michelle Y. Wang, Huijuan Jiang, Tint Lwin, Paul M. Park, Jing Gao, Mark B. Meads, Yuan Ren, Tao Li, Jiao Sun, Naima Ahmed Fahmi, Satishkumar Singh, Lalit Sehgal, Xuefeng Wang, Ariosto S. Silva, Eduardo M. Sotomayor, Kenneth H. Shain, John L. Cleveland, Michael Wang, Wei Zhang, Jun Qi, Bijal D. Shah, and Jianguo Tao

Figure S1

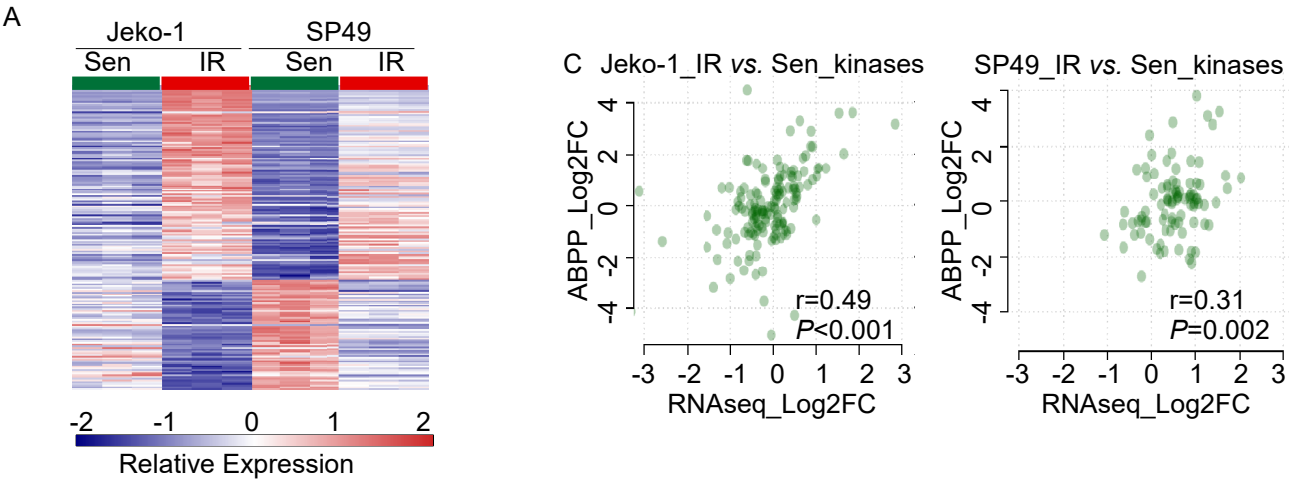

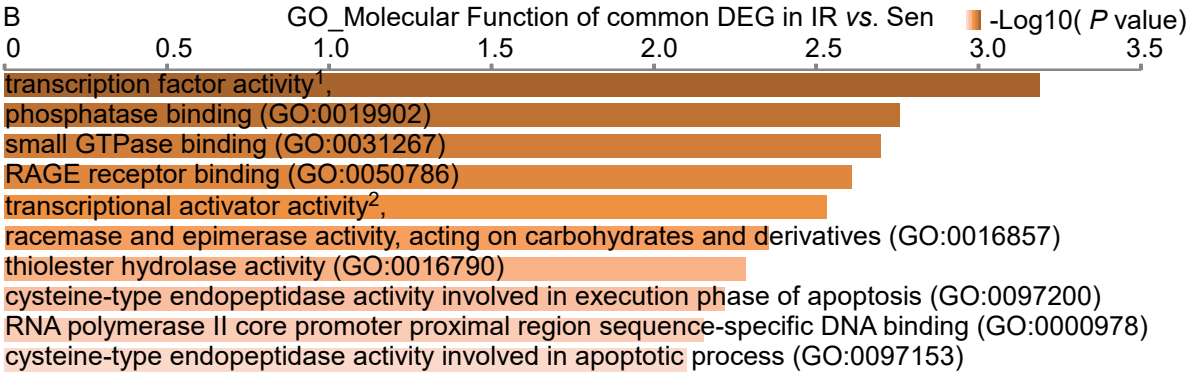

[1]. RNA polymerase II core promoter proximal region sequence-specific binding (GO:0000982)
[2].RNA polymerase II transcription regulatory region sequence-specific binding (GO:0001228)

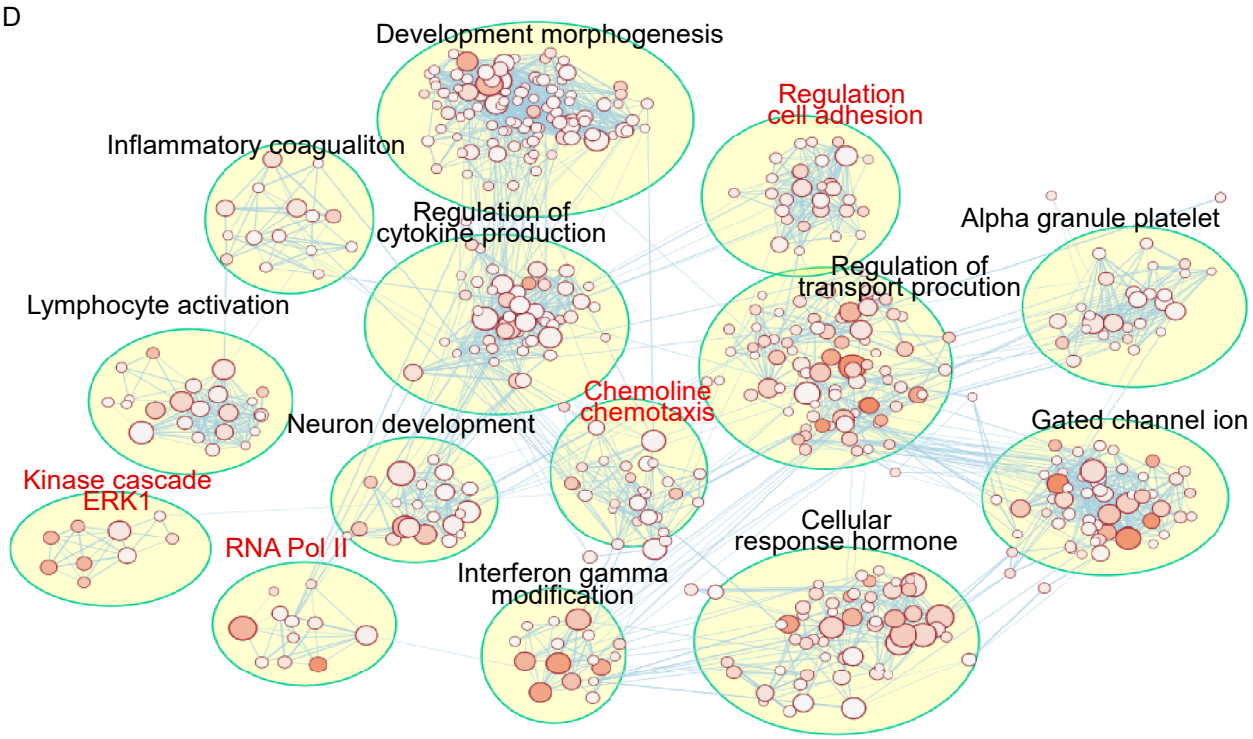

Figure S1 (Related to Figure 1). Transcriptome Reprograming Rewires Kinome Signaling in Ibrutinib Resistant (IR) Mantle Cell Lymphoma (MCL). A, Heatmap showing common significant differential gene expression profiles in IR cells (Jeko-1-IR and SP49-IR) vs their Sen parental cell lines in biological triplicate. **B,** GO term Molecular function analysis of common differential expressed genes (from figure S1A). Bar length and top axis represent -log10(*P* value). Color bar intensity represents -log10(*P* value) where the darker colors are indicative of higher significance (lower *P* value). **C,** Correlation between differential mRNA expression and kinase activities of IR *vs.* Sen Jeko-1 and SP49 cells. Log2 fold change of mRNA and kinase expression between paired IR and Sen Jeko-1 and SP49 cells are shown. RNA-seq data are from triplicate samples and ABPP data are from three or four replicates. **D,** Enrichment map of IR-associated genes in SP49-IR cells. The map displays the enriched gene-sets in SP49-IR cells. Nodes represent gene-sets and edges represent overlap between gene-sets. Gene-sets that did not pass the enrichment significance threshold are not shown. Clusters of functionally related gene-sets were assigned a label using “AutoAnnotate” Add-in in Cytoscape; node color intensity is proportional to enrichment significance, clusters of biological and functional interest for their role in IR are highlighted in red.

Figure S2

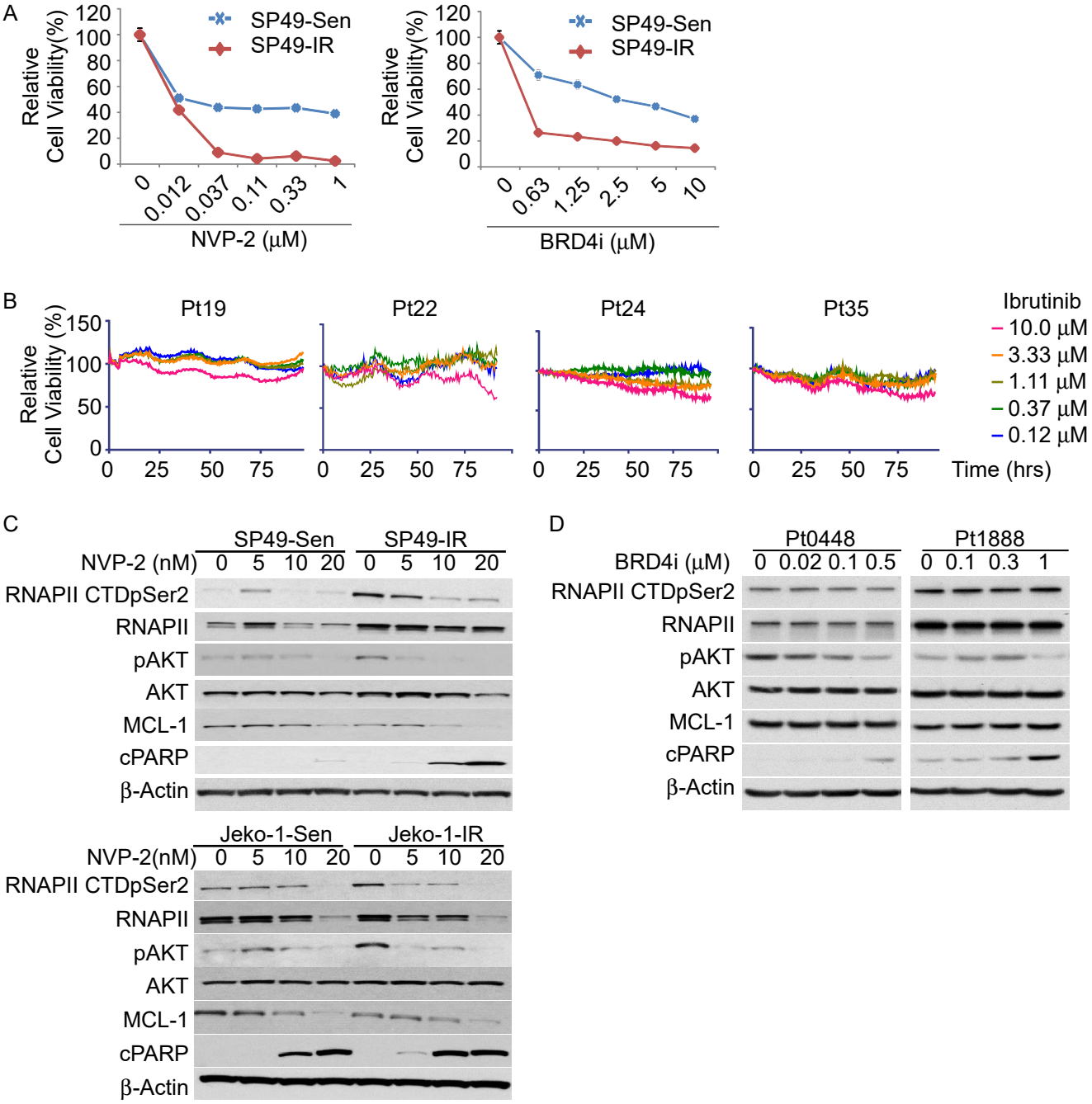
A
Relative Cell Viability(%)
120
100
80
60
40
20
0
SP49-Sen
SP49-IR
0
0.012
0.037
0.11
0.33
1
NVP-2 (μM)
Relative Cell Viability(%)
SP49-Sen
SP49-IR
0
0.63
1.25
2.5
5
10
BRD4i (μM)
B
Relative Cell Viability (%)
150
100
50
0
Pt19
Pt22
Pt24
Pt35
0
25
50
75
Time (hrs)
Ibrutinib
10.0 μM
3.33 μM
1.11 μM
0.37 μM
0.12 μM
C
SP49-Sen
SP49-IR
NVP-2 (nM)
0 5 10 20 0 5 10 20
RNAPII CTDpSer2
RNAPII
pAKT
AKT
MCL-1
cPARP
β-Actin
Jeko-1-Sen
Jeko-1-IR
NVP-2(nM)
0 5 10 20 0 5 10 20
RNAPII CTDpSer2
RNAPII
pAKT
AKT
MCL-1
cPARP
β-Actin
D
Pt0448
Pt1888
BRD4i (μM)
0 0.02 0.1 0.5
0 0.1 0.3 1
RNAPII CTDpSer2
RNAPII
pAKT
AKT
MCL-1
cPARP
β-Actin

Figure S2 (Related to Figure 2). Ibrutinib Resistant (IR) Mantle Cell Lymphoma (MCL) Cells Are Highly Sensitive to CDK9 Inhibition. A, Cell viability assay shows the dose response of NVP-2 (left) and INCB054329 (right) in paired IR and Sen parental cells. **B**, Drug response assessment of primary MCL specimens treated with the indicated doses of Ibrutinib. **C,** NVP-2 treatment induced more suppression of phosphorylation of the C-terminal repeat domain (CTD) of RNA polymerase II (RNAPII) at the large subunit of RNAPII on Ser2, pAKT, and MCL-1 levels, and induced more PARP cleavage in IR compared to Sen cells. **D**, INCB054329 induced suppression of pAKT and MCL-1 and increased PARP cleavage in primary MCL patient samples (Pt0448, Pt1888). Data in A, C and D are representative of 3 independent experiments.

Figure S3

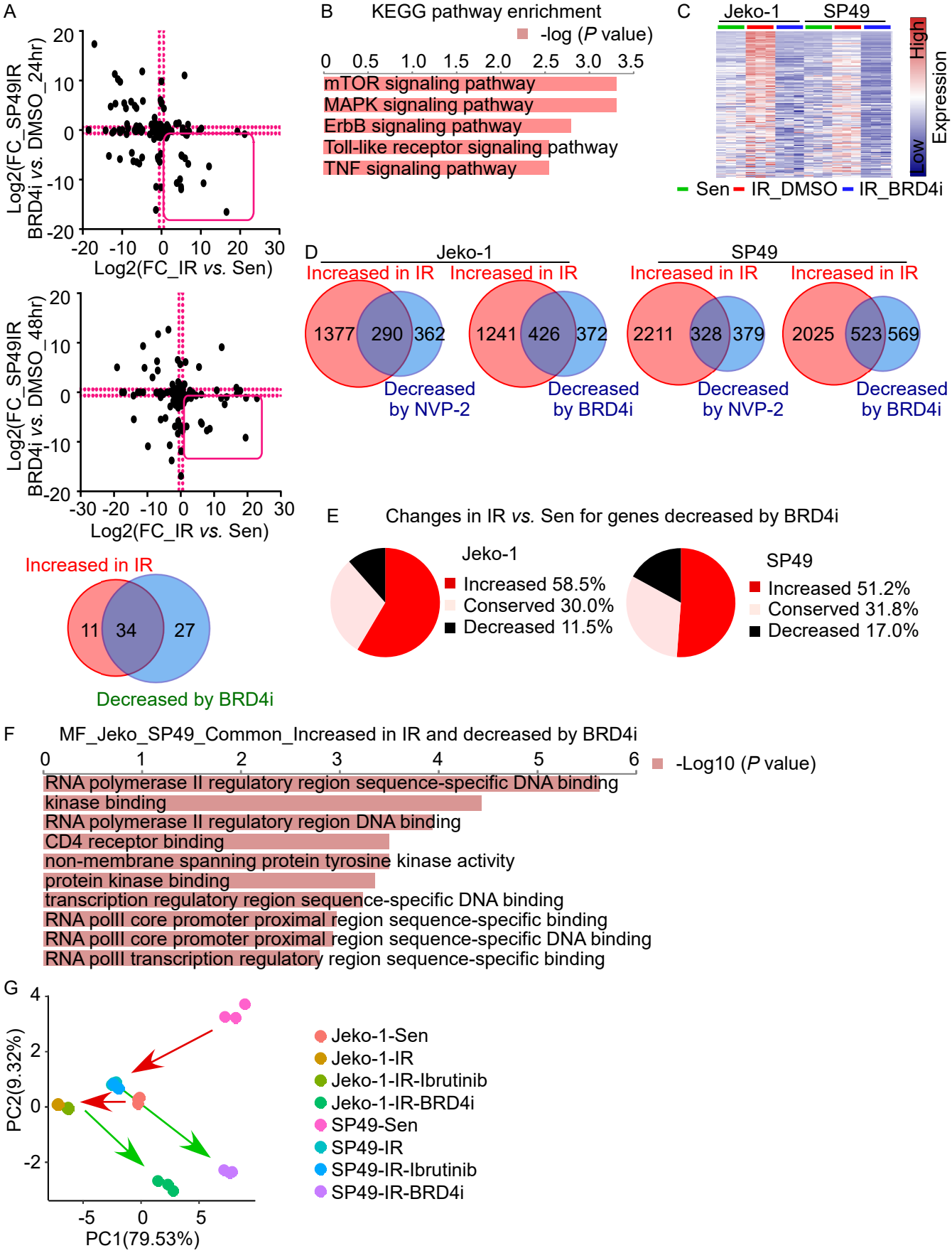
A
Log2(FC_SP49IR BRD4i vs. DMSO_24hr)
Log2(FC_IR vs. Sen)
Log2(FC_SP49IR BRD4i vs. DMSO_48hr)
Log2(FC_IR vs. Sen)
Increased in IR
11 34 27
Decreased by BRD4i
B KEGG pathway enrichment
-log (P value)
mTOR signaling pathway
MAPK signaling pathway
ErbB signaling pathway
Toll-like receptor signaling pathway
TNF signaling pathway
C Jeko-1 SP49
High
Low
Expression
Sen IR_DMSO IR_BRD4i
D Jeko-1
Increased in IR Increased in IR
1377 290 362
Decreased by NVP-2
1241 426 372
Decreased by BRD4i
SP49
Increased in IR Increased in IR
2211 328 379
Decreased by NVP-2
2025 523 569
Decreased by BRD4i
E Changes in IR vs. Sen for genes decreased by BRD4i
Jeko-1
Increased 58.5%
Conserved 30.0%
Decreased 11.5%
SP49
Increased 51.2%
Conserved 31.8%
Decreased 17.0%
F MF_Jeko_SP49_Common_Increased in IR and decreased by BRD4i
-Log10 (P value)
RNA polymerase II regulatory region sequence-specific DNA binding
kinase binding
RNA polymerase II regulatory region DNA binding
CD4 receptor binding
non-membrane spanning protein tyrosine kinase activity
protein kinase binding
transcription regulatory region sequence-specific DNA binding
RNA polII core promoter proximal region sequence-specific binding
RNA polII core promoter proximal region sequence-specific DNA binding
RNA polII transcription regulatory region sequence-specific binding
G
PC2(9.32%)
PC1(79.53%)
Jeko-1-Sen
Jeko-1-IR
Jeko-1-IR-Ibrutinib
Jeko-1-IR-BRD4i
SP49-Sen
SP49-IR
SP49-IR-Ibrutinib
SP49-IR-BRD4i

Figure S3 (Related to Figure 3). CDK9 Is Required to Sustain Transcriptional and Kinase Reprogramming in Ibrutinib Resistant (IR) Mantle Cell Lymphoma (MCL) Cells. A, Fold change in kinase activity in IR *vs.* Sen SP49 cells (*x*-axes), and in SP49-IR cells treated with BRD4i INCB054329 (y-axes; 24hrs [top] or 48hr [middle]). Venn diagram at bottom shows the overlap between kinases whose activity is increased in IR cells and decreased by INCB054329 treatment. These overlapped kinases are highlighted by the red box in each scatterplot. Cutoff, FC=1.5. n = 3 biological replicates. **B**, KEGG pathway enrichment of kinases whose activity is increased in IR compared to Sen MCL cells, and that also decreased by INCB054329 treatment in IR cells. Top axis and bar length represent -log10(*P* value). **C**, RNAseq heatmap of genes that are increased in IR compared to Sen and that are decreased by INCB054329 treatment. n = 3 biological replicates. **D**, Venn diagrams show the overlap between IR specific genes and genes decreased by NVP-2 or INCB054329 treatment in IR cells. **E**, Pie chart showing the percentage of gene expression changes (increase/conserved/decrease) in IR compared to Sen cells for INCB054329 decreased genes in IR cells. More than half (58.5% for Jeko-1 and 51.2% for SP49) of the INCB054329 decreased genes are increased in IR cells compared to sensitive cells. **F**, Molecular function enrichment results by Enrichr for genes in (D). Top axis and bar length represent -log10(*P* value). **G**, PCA analysis of RNA-seq data showing that IR cells are distinct from Sen cells and that Ibrutinib treated IR cells cluster with IR cells treated with vehicle (DMSO). In contrast, INCB054329 treatment of IR MCL cells provokes a shift towards Sen cell clusters. n = 3 biological replicates.

Figure S4

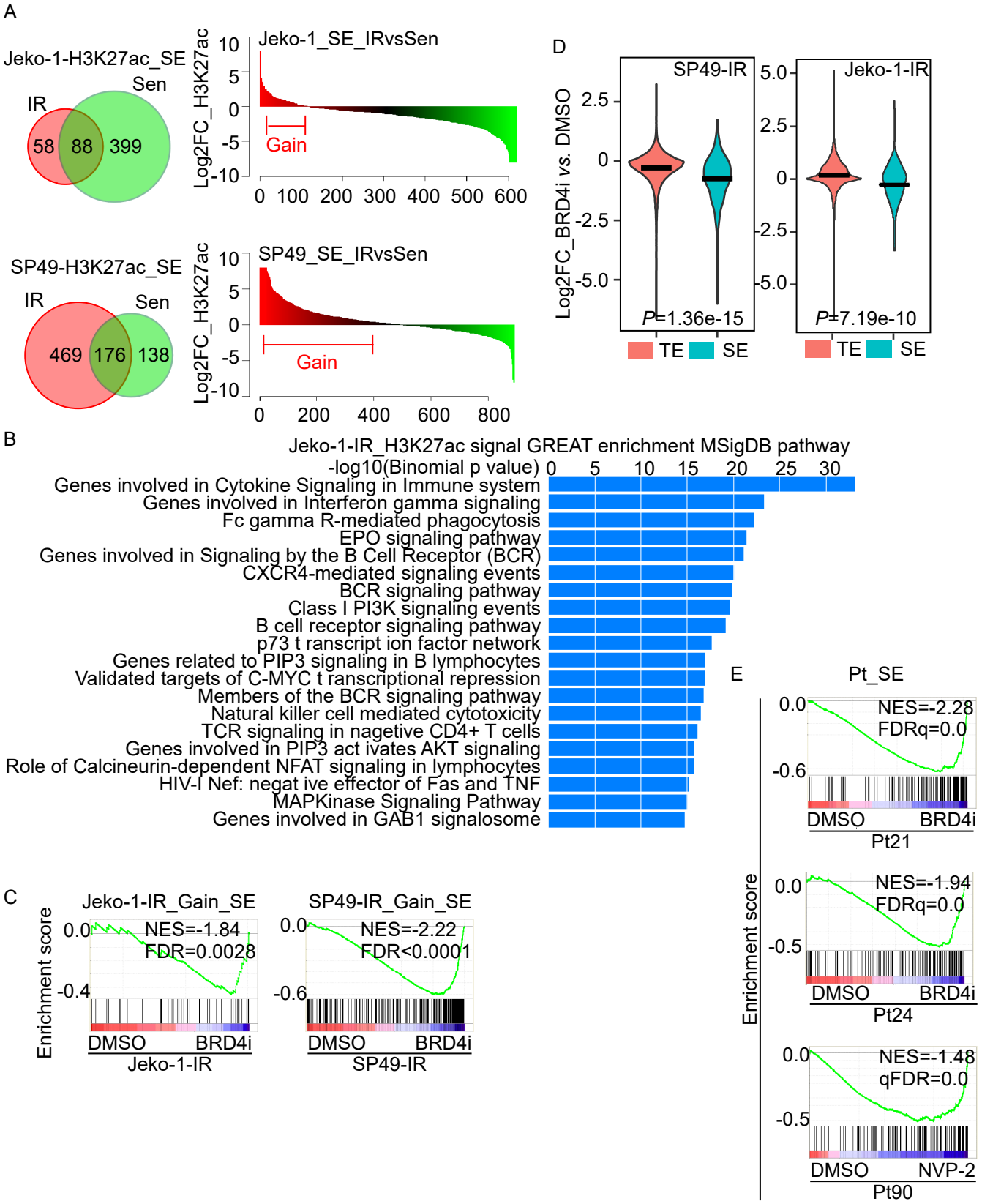
A
Jeko-1-H3K27ac_SE
IR
Sen
58
88
399
Jeko-1_SE_IRvsSen
Log2FC_H3K27ac
Gain
SP49-H3K27ac_SE
469
176
138
SP49_SE_IRvsSen
D
SP49-IR
Jeko-1-IR
Log2FC_BRD4i vs. DMSO
P=1.36e-15
P=7.19e-10
TE
SE
B
Jeko-1-IR_H3K27ac signal GREAT enrichment MSigDB pathway
-log10(Binomial p value)
Genes involved in Cytokine Signaling in Immune system
Genes involved in Interferon gamma signaling
Fc gamma R-mediated phagocytosis
EPO signaling pathway
Genes involved in Signaling by the B Cell Receptor (BCR)
CXCR4-mediated signaling events
BCR signaling pathway
Class I PI3K signaling events
B cell receptor signaling pathway
p73 t ranscript ion factor network
Genes related to PIP3 signaling in B lymphocytes
Validated targets of C-MYC t ranscriptional repression
Members of the BCR signaling pathway
Natural killer cell mediated cytotoxicity
TCR signaling in nagetive CD4+ T cells
Genes involved in PIP3 act ivates AKT signaling
Role of Calcineurin-dependent NFAT signaling in lymphocytes
HIV-I Nef: negat ive effector of Fas and TNF
MAPKinase Signaling Pathway
Genes involved in GAB1 signalosome
C
Jeko-1-IR_Gain_SE
SP49-IR_Gain_SE
Enrichment score
NES=-1.84
FDR=0.0028
NES=-2.22
FDR<0.0001
DMSO
BRD4i
Jeko-1-IR
SP49-IR
E
Pt_SE
NES=-2.28
FDRq=0.0
Pt21
NES=-1.94
FDRq=0.0
Pt24
NES=-1.48
qFDR=0.0
NVP-2
Pt90

Figure S4 (Related to Figure 4). Super-Enhancer (SE) Remodeling Drives Transcriptional Programming and Drug Sensitivity to CDK9 Inhibition in Ibrutinib Resistant (IR) Mantle Cell Lymphoma (MCL) lines and Primary Samples. A, Venn diagram (left) and waterfall (right) plot showing overlap and specific SE in paired IR and Sen parental Jeko-1 (top) and SP49 (bottom) MCL cells. **B,** Genomic Regions Enrichment of Annotations Tool (GREAT) analysis of Jeko-1-IR H3K27ac enrichment. **C**, Gene Set Enrichment Analysis (GSEA) shows gained SE regulated genes are decreased by INCB054329 treatment in Jeko-1-IR and SP49-IR cells. **D**, Box plots showing Log2 fold changes of gene expression following INCB054329 treatment *vs.* vehicle (DMSO) in Jeko-1-IR and SP49-IR cells. Typical enhancer (TE) or SE associated genes are defined by the density and amplitude of H3K27ac marks from ChIP-seq analyses. Significance was determined using the Kruskal-Wallis test; SP49 *P* = 1.36e-15; Jeko-1 *P* = 7.19e-10. **E**, GSEA shows SE regulated genes are decreased by INCB054329 or NVP-2 treatment in primary IR MCL samples. NES, normalized enrichment score; FDR, false discovery rate.

Figure S5

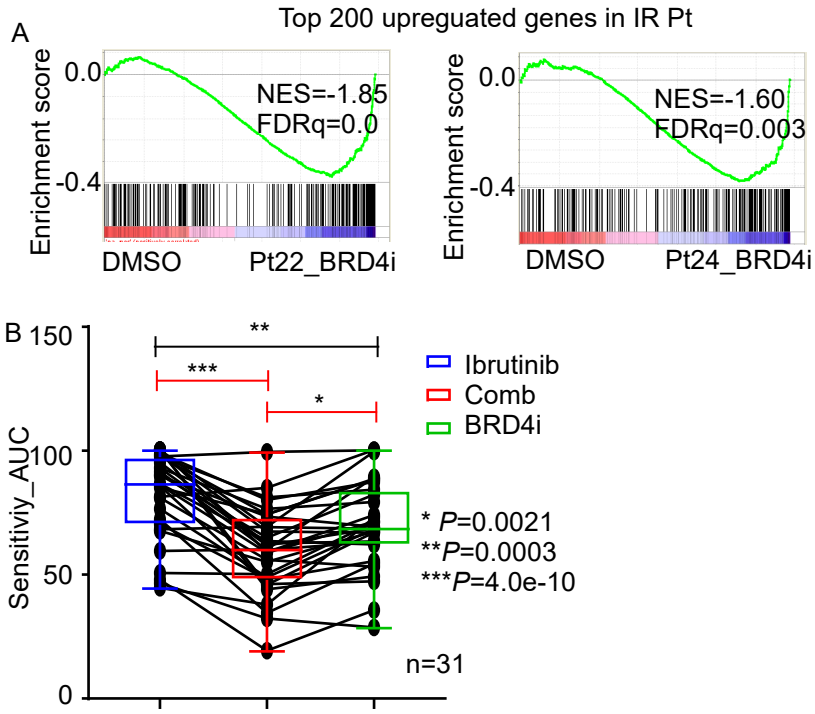
A
Top 200 upreguated genes in IR Pt
Enrichment score
0.0
-0.4
NES=-1.85
FDRq=0.0
DMSO
Pt22_BRD4i
Enrichment score
0.0
-0.4
NES=-1.60
FDRq=0.003
DMSO
Pt24_BRD4i
B
150
100
50
0
Sensitiviy_AUC
**
***
*
Ibrutinib
Comb
BRD4i
* P=0.0021
**P=0.0003
***P=4.0e-10
n=31

Figure S5 (Related to Figure 5). Targeting CDK9 Prevents Emergence and Overcomes Ibrutinib Resistance (IR) in Mantle Cell Lymphoma (MCL) *ex vivo* and *in vivo*. A, Gene Set Enrichment Analysis (GSEA) of differential gene expression shows top 200 upregulated genes in IR primary MCL patient samples are negatively enriched by INCB054329 treatment. NES, normalized enrichment score; FDR, false discovery rate. **B,** Drug response assay of primary MCL patient samples treated with Ibrutinib or INCB054329 alone or the Ibrutinib/INCB054329 combination by AUC measured by cell-based imaging analysis. *P* values were calculated by one-way ANOVA. n = 31 primary MCL patient samples.

Figure S6

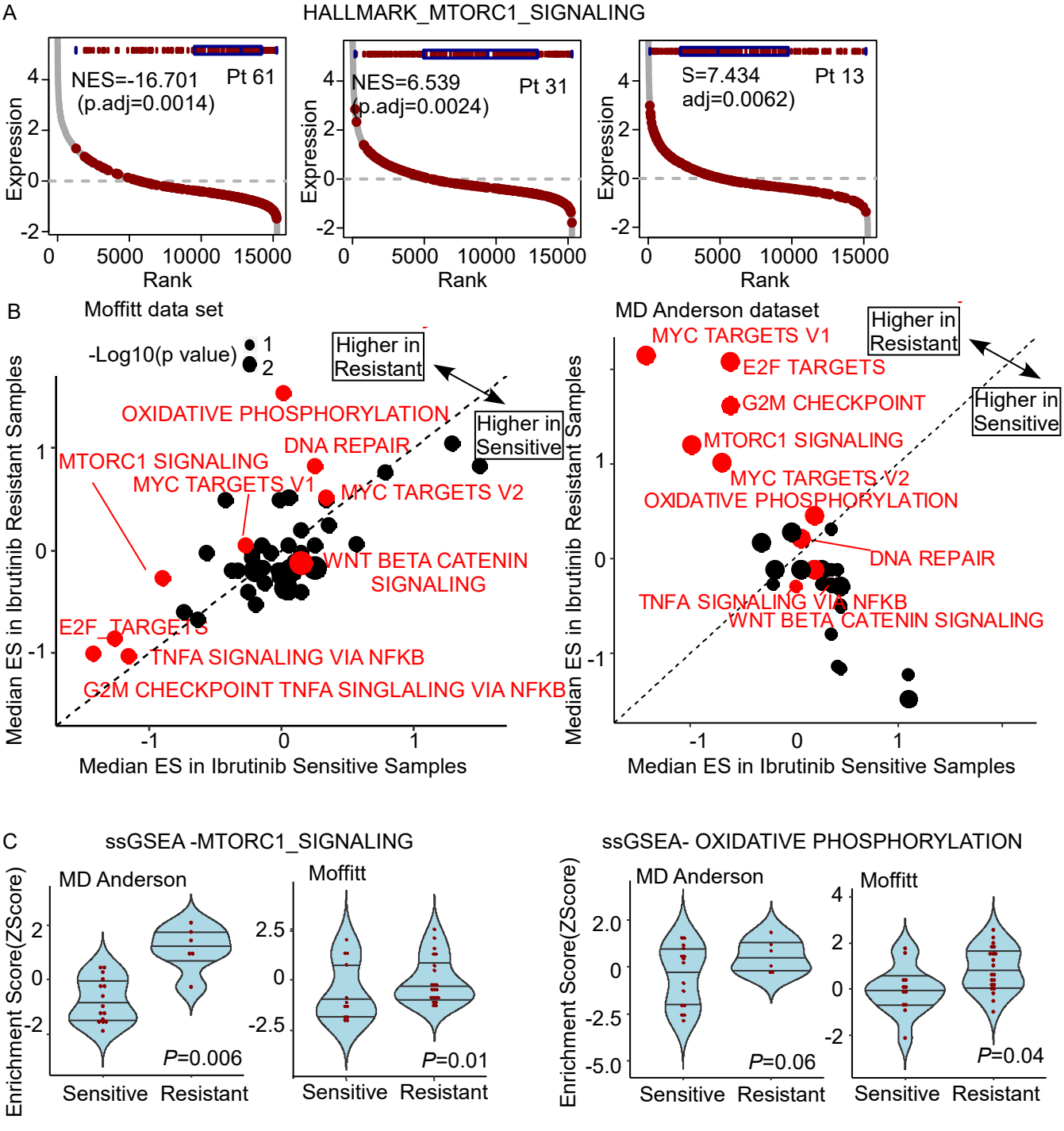
A
HALLMARK_MTORC1_SIGNALING
NES=-16.701
(p.adj=0.0014)
Pt 61
NES=6.539
(p.adj=0.0024)
Pt 31
S=7.434
adj=0.0062)
Pt 13
Expression
Rank
B
Moffitt data set
-Log10(p value)
Higher in Resistant
Higher in Sensitive
OXIDATIVE PHOSPHORYLATION
DNA REPAIR
MTORC1 SIGNALING
MYC TARGETS V1
MYC TARGETS V2
WNT BETA CATENIN SIGNALING
E2F_TARGETS
TNFA SIGNALING VIA NFKB
G2M CHECKPOINT TNFA SINGLALING VIA NFKB
Median ES in Ibrutinib Resistant Samples
Median ES in Ibrutinib Sensitive Samples
MD Anderson dataset
MYC TARGETS V1
E2F TARGETS
G2M CHECKPOINT
MTORC1 SIGNALING
MYC TARGETS V2
OXIDATIVE PHOSPHORYLATION
DNA REPAIR
TNFA SIGNALING VIA NFKB
WNT BETA CATENIN SIGNALING
C
ssGSEA -MTORC1_SIGNALING
MD Anderson
Moffitt
Enrichment Score(ZScore)
P=0.006
P=0.01
Sensitive
Resistant
ssGSEA- OXIDATIVE PHOSPHORYLATION
P=0.06
P=0.04

Figure S6 (Related to Figure 6). The EMMA Platform Predicts Clinical Responses and Informs Vulnerabilities in Primary and Ibrutinib Resistant (IR) Mantle Cell Lymphoma (MCL). A, Single-sample gene set enrichment analysis (ssGSEA) of representative primary MCL samples for mTORC1_SIGNALING Negative enrichment in Ibrutinib sensitive MCL samples (left panel, Pt 61), positive enrichment in IR MCL samples (right panel, Pt 13) and intermediate enrichment (middle panel, Pt 31). **B**, ssGSEA of enriched pathways in IR versus sensitive MCL patients from the MD Anderson (right) and Moffitt (left) datasets were performed, and the resulting enrichment scores were compared between IR and Sen patient groups. The Ibrutinib sensitivity groups were defined by maximal Ibrutinib effect measured by cell-based imaging analysis for Moffitt datasets and clinical response for MD Anderson datasets. Note the red highlighted circles indicate higher enrichment scores for MYC, NF-κB and mTOR pathways in IR MCL patient samples, and higher enrichment scores for WNT and DNA repair pathways in Ibrutinib sensitive MCL patient samples of both datasets. **C**, ssGSEA reveals higher enrichment score for the mTORC1 and OXIDATIVE PHOSPHORYLATION pathway HALLMARK signatures in resistant compared to sensitive primary patient sample for both MD Anderson and Moffitt datasets. Ibrutinib sensitivity groups are defined as in B.